AN OVER-COMPLETE DICTIONARY BASED REGULARIZED RECONSTRUCTION OF A FIELD OF ENSEMBLE AVERAGE PROPAGATORS

Wenxing Ye, Baba C. Vemuri, Alireza Entezari

CISE Department, University of Florida, Gainesville, FL 32611-6120, USA

ABSTRACT

In this paper we present a dictionary-based framework for the reconstruction of a field of ensemble average propagators (EAPs), given a high angular resolution diffusion MRI data set. Existing techniques often consider voxel-wise reconstruction of the EAP field thereby leading to a noisy reconstruction across the field. We present a dictionary learning framework for achieving a smooth EAP reconstruction across the field wherein, the dictionary atoms are learned from the data via an initial regression using adaptive spline kernels. The formulation involves a two stage optimization where the first stage involves optimizing for a sparse dictionary using a K-SVD based updating and the second stage involves a quadratic cost function optimization with a non-local means based regularization across the field. The novelty lies in a dictionary based reconstruction as well as an NLM-based regularization that helps preserving features in the reconstructed field. We document experimental results on synthetic data from crossing fibers and real optic chiasm data set that demonstrate the advantages of the proposed approach.

Index Terms— Diffusion Propagator, DW-MRI, Sparse representation, Dictionary learning.

1. INTRODUCTION

Diffusion weighted MRI is a non-invasive imaging technique which tells the connectivity patterns of fibrous tissues through sensing the Brownian motion of water molecules. One of the major tasks of diffusion MRI is the reconstruction of the 3-D diffusion ensemble average propagator (EAP), $P(\boldsymbol{r})$, which characterizes the diffusion of water molecules with a probability density function (PDF) defined at each voxel. $P(\boldsymbol{r})$ cannot be measured directly. Instead, the diffusion signal, $S(\boldsymbol{q})$, is sensed by the scanner. Under the narrow pulse assumption, the diffusion signal in $\boldsymbol{q}$-space and the diffusion propagator in displacement ($\boldsymbol{r}$) space are related through the Fourier transform [1]:

$$P(\boldsymbol{r}) = \int E(\boldsymbol{q}) \exp(-2\pi i \boldsymbol{q} \cdot \boldsymbol{r}) \mathrm{d}\boldsymbol{q} \qquad (1)$$

This research was supported by the NIH grant NS066340 to Baba Vemuri and the NSF grant CCF-1018149, IIS-1048508 to Alireza Entezari.

where $E(\boldsymbol{q}) = S(\boldsymbol{q})/S_0$, $S_0 = S(\boldsymbol{0})$.

Various techniques have been proposed to reconstruct $P(\boldsymbol{r})$ from samples of $S(\boldsymbol{q})$. Diffusion tensor imaging (DTI) [2] is a simple method which characterizes the diffusion propagator using an oriented Gaussian function. It is now well know that this model fails to capture multi-fiber structure with more than one fiber orientations within one voxel. To overcome the limitation of DTI, high angular resolution diffusion imaging (HARDI) [3] was proposed where $S(\boldsymbol{q})$ is measured on a single shell in the $\boldsymbol{q}$-space. It is possible to fit more sophisticated models to the signal such as a mixture of Gaussian densities [3]. Other techniques include diffusion orientation transform (DOT) [4], diffusion propagator imaging [5], tomographic reconstruction methods [6] and spherical deconvolution [7].

The DW-MRI datasets are usually provided as a field of $S(\boldsymbol{q}, \boldsymbol{x})$ where $\boldsymbol{x}$ specifies spatial locations. Most of the existing reconstruction methods reconstruct $P(\boldsymbol{r}, \boldsymbol{x})$ at each location $\boldsymbol{x}$ independently which do not consider the spatial coherency that inherently exists in the data. In a recent study [8], a spatially regularized reconstruction approach was developed that exploits sparse representation of $P(\boldsymbol{r})$ in spherical ridgelet basis. In this framework, spherical ridgelet transform was applied at every voxel on $S(\boldsymbol{q}, \boldsymbol{x})$ to obtain a sparse representation. Then the sparsity of transform-domain coefficients as well as the total variation of the reconstructed signal field $S(\boldsymbol{q}, \boldsymbol{x})$, with respect to $\boldsymbol{x}$ were used to formulate the reconstruction as the following optimization problem:

$$\min_{\boldsymbol{C}} \frac{1}{2} ||\boldsymbol{AC} - \boldsymbol{S}||_F^2 + \lambda \sum_i ||\boldsymbol{c}_i||_1 + \mu TV\{\boldsymbol{AC}\}. \qquad (2)$$

In this formulation, $\boldsymbol{A}$ is the spherical ridgelet transform matrix, $\boldsymbol{C}$ contains the transform coefficients at all voxels in the field of interest where each column, $\boldsymbol{c}_i$, is one set of transform coefficients at i^{th} voxel. $\boldsymbol{AC}$ represents the reconstructed diffusion signal field and $TV\{\boldsymbol{AC}\}$ is the total variation of the reconstructed field. The third term enforces correlations among $\boldsymbol{c}_i$ from neighbouring voxels which makes the solution of the coefficient field spatially regularized. The final step is to calculate the diffusion propagator from the reconstructions as $\boldsymbol{P} = \mathscr{F}\{\boldsymbol{A}\}\boldsymbol{C}$ where $\mathscr{F}\{\boldsymbol{A}\}$ denotes the Fourier transform of the basis functions (i.e., spherical ridgelets).

$\boldsymbol{A}$ in the above formulation is fixed to be the spherical ridgelet bases truncated up to a certain degree. In contrast we introduce a dictionary-based method where we learn the basis functions in $\boldsymbol{A}$ from data examples that will provide a sparse representation. Through updating both $\boldsymbol{A}$ and $\boldsymbol{C}$ during the optimization process, we obtain a dictionary learned from the specific dataset as well as the corresponding sparse representation of the reconstruction. The globally defined dictionary plays an implicit role of regularizing the reconstructions over different voxels. We also introduce the spherical deconvolution model with adaptive kernels to control the way the dictionary gets updated. In addition, we use an NLM-based regularization which further suppresses the noise. We will briefly introduce the adaptive kernels in Section 2 and give the dictionary learning framework in Section 3. Section 4 will show the experiment results and Section 5 is the conclusion section.

2. ADAPTIVE KERNELS FOR MULTI-FIBER RECONSTRUCTION

Given a diffusion-weighted MR dataset, there are many methods employing different spherical deconvolution kernels to reconstruct the multi-fiber diffusion profile. In the spherical deconvolution framework, the DW-MRI signal is considered as the convolution of a kernel function k with a probability density function f over the sphere [7]:

$$E(b, \boldsymbol{g}) = \int f(\boldsymbol{p}) k(b, \boldsymbol{g}|\boldsymbol{p}) \, \mathrm{d}\boldsymbol{p} \tag{3}$$

where b is the diffusion weighting, $||\boldsymbol{g}|| = 1$ and $\boldsymbol{q} \sim \sqrt{b}\boldsymbol{g}$. The integration is over the domain of parameter $\boldsymbol{p}$. Many well known reconstruction techniques turn out to be the special cases of Equation 3 by picking certain kernel functions $k(b, \boldsymbol{g}|\boldsymbol{p})$ and mixing densities $f(\boldsymbol{p})$ [7]. For example, k can be multivariate Gaussian function $k(b, \boldsymbol{g}|\boldsymbol{D}) = \exp(-b\boldsymbol{g}^T \boldsymbol{D}\boldsymbol{g})$[9]. The choices of such fix-shaped kernels are used to represent the diffusion property of the underlying fibers; however they also impose some unnecessary assumptions which may not hold for the real DW-MRI dataset.

Adaptive spline kernels [10] were proposed as a flexible kernel model to fit datasets with varieties of different diffusion patterns. The density function f is re-parametrized on the sphere as $f(\boldsymbol{p}) = \sum_{j=1}^{N} w_j \phi(\boldsymbol{p}|\boldsymbol{v}_j)$ where $\boldsymbol{v}_1, ..., \boldsymbol{v}_N$ is a set of unit vectors uniformly distributed on the hemisphere. By letting the reconstruction kernel $K(b, \boldsymbol{g}|\boldsymbol{v}_j) = \int \phi(\boldsymbol{p}|\boldsymbol{v}_j) k(b, \boldsymbol{g}|\boldsymbol{p}) \mathrm{d}\boldsymbol{p}$ and considering the case of a constant b-value (which is quite common in HARDI acquisition), we have:

$$E(\boldsymbol{g}) = \sum_{j=1}^{N} w_j K(\boldsymbol{g}|\boldsymbol{v}_j) = \sum_{j=1}^{N} w_j \sum_{k=1}^{P} c_k \psi_k(|\boldsymbol{g} \cdot \boldsymbol{v}_j|), \tag{4}$$

where K is represented in spline bases ψ_k. The shape of the kernel is flexible and is determined by the control points c_k. When we plug a number of measurements $S(\boldsymbol{g_i}), i = 1, ..., M$ and the corresponding gradient directions $\boldsymbol{g}_i$ into Equation 4, we obtain M linear equations with respect to unknowns w_j and c_k. w_j and c_k are then estimated through non-negative least square fitting in an alternative pattern. In other words, w_j is estimated while c_k are fixed and then c_k's are estimated while w_j are fixed. See [10] for details of the search algorithm.

Finally, the diffusion propagator is calculated by the estimated w_j and c_k parameters and by applying the Fourier transform on both sides of Equation 4. Since ψ_k are known spline bases, their Fourier transforms can be calculated beforehand.

3. DICTIONARY BASED RECONSTRUCTION FRAMEWORK

In the afore-mentioned spherical deconvolution framework, diffusion signal is modelled as weighted sum of kernel functions each of which represents the diffusion properties of a single fiber. The number of parameters, c_k, in kernel functions and the weights, w_j, is usually very large which makes the reconstruction problem ill-posed. Fortunately, the fact that the number of fibers at each voxel is limited in real datasets allows us to exploit the sparsity of weighting coefficients to solve the reconstruction problem. The problem of searching for the proper kernel function as well as the sparse weighting coefficients can be solved by a dictionary learning paradigm.

For a given voxel v, we define the weights as a vector $\boldsymbol{w}_v$ whose j^{th} element is denoted by w_j, the measurements as vector $\boldsymbol{e}_v$ whose i^{th} element is denoted by $E(\boldsymbol{g}_i)$, and $\boldsymbol{K}_v$ which denotes the kernel $\boldsymbol{K}_v(i, j) = K(\boldsymbol{g}_i|\boldsymbol{v}_j)$. With these notations Equation 4 becomes $\boldsymbol{e}_v = \boldsymbol{K}_v \boldsymbol{w}_v$ where $\boldsymbol{K}$ is flexible by changing coefficients c_k. Modelling signal within a single voxel can be interpreted as a dictionary learning problem with one observation and dictionary atoms formed by our splines.

Instead of fitting the adaptive kernel to the signal at each voxel individually, here we use an over complete dictionary $\boldsymbol{K}_{M \times D}, D > N$ for all the voxels. We define $\boldsymbol{E} = [\boldsymbol{e}_1, ..., \boldsymbol{e}_V]$ as the measurements from all the voxels in the field of interest, $\boldsymbol{W} = [\boldsymbol{w}_1, ..., \boldsymbol{w}_v]$ as the corresponding weights respect to the new global dictionary $\boldsymbol{K}$. Now, we can formulate the modelling of the whole field as the optimization problem:

$$\min_{\boldsymbol{K}, \boldsymbol{W}} ||\boldsymbol{E} - \boldsymbol{K}\boldsymbol{W}||_F^2 \text{ s.t. } \forall v, ||\boldsymbol{w}_v||_0 \leq T_0 \tag{5}$$

where T_0 specifies how many non-zero weights are allowed. There are many algorithms which solve this dictionary learning problem, we pick the K-SVD algorithm [11] because of its simplicity and efficiency. The global dictionary $\boldsymbol{K}$ implicitly brings in some spatial regularization such that the reconstructed field $\boldsymbol{K}\boldsymbol{W}$ does not change independently at each voxel. The dictionary size D and sparsity constraint T_0 indirectly control the smoothness of the reconstructions.

In order to further suppress the noise during the reconstruction, we introduce an explicit regularization term:

$$\min_{\boldsymbol{K},\boldsymbol{W}} ||\boldsymbol{E}-\boldsymbol{K}\boldsymbol{W}||_F^2+\gamma\sum_v ||\boldsymbol{w}_v||_0+\mu\mathscr{M}\{\boldsymbol{K}\boldsymbol{W}\} \quad (6)$$

where $\mathscr{M}\{\boldsymbol{K}\boldsymbol{W}\}$ is a roughness measure of the reconstruction $\boldsymbol{K}\boldsymbol{W}$. In Equation 2, $\mathscr{M}$ is set to be the total variation. In this paper, we propose to use the deviation of $\boldsymbol{K}\boldsymbol{W}$ from its non-local means $NL\{\boldsymbol{K}\boldsymbol{W}\}$ [12], i.e. $\mathscr{M}\{\boldsymbol{K}\boldsymbol{W}\} = ||\boldsymbol{K}\boldsymbol{W}-NL\{\boldsymbol{K}\boldsymbol{W}\}||_F^2$.

A direct solution to this problem is difficult because of the complicated regularization term. We split the original problem into two sub-problems by introducing an auxiliary variable $\boldsymbol{Y}=\boldsymbol{K}\boldsymbol{W}$ and solve them using an alternating method. With the auxiliary variable included, the original problem can be written as:

$$\min_{\boldsymbol{K},\boldsymbol{W}} ||\boldsymbol{E}-\boldsymbol{Y}||_F^2+\gamma\sum_v ||\boldsymbol{w}_v||_0+\mu\mathscr{M}\{\boldsymbol{Y}\}+\lambda||\boldsymbol{Y}-\boldsymbol{K}\boldsymbol{W}||_F^2 \quad (7)$$

At each iteration t, we are solving the following two problems:

$$\textit{Step 1} \quad \{\boldsymbol{K}^t,\boldsymbol{W}^t\}=\arg\min_{\boldsymbol{K},\boldsymbol{W}} ||\boldsymbol{Y}^t-\boldsymbol{K}\boldsymbol{W}||_F^2 \quad (8)$$
$$\text{s.t. } \forall v, ||\boldsymbol{w}_v||_0 \le T_0$$
$$\textit{Step 2} \quad \boldsymbol{Y}^{t+1}=\arg\min_{\boldsymbol{Y}} ||\boldsymbol{Y}-\boldsymbol{E}||_F^2+\lambda||\boldsymbol{Y}-\boldsymbol{K}^t\boldsymbol{W}^t||_F^2$$
$$+\mu||\boldsymbol{Y}-NL\{\boldsymbol{K}^t\boldsymbol{W}^t\}||_F^2 \quad (9)$$

The problem in setp 2 is actually a quadratic problem which has a closed form solution:

$$\boldsymbol{Y}^{t+1}=(\boldsymbol{E}+\lambda\boldsymbol{K}^t\boldsymbol{W}^t+\mu NL\{\boldsymbol{K}^t\boldsymbol{W}^t\})/(1+\lambda+\mu) \quad (10)$$

To initialize the dictionary $\boldsymbol{K}$, we individually fit the adaptive spline kernel to every voxel in the field and pick D of the kernels with the largest weights across the field. And at each iteration t, we refit the adaptive kernel to $\boldsymbol{K}^t$ to ensure that the atoms of our dictionary can still be expressed in Equation 4.

4. EXPERIMENTS

In this section, we evaluate our proposed reconstruction framework by comparing to the reconstruction of $P(\boldsymbol{r})$ on individual voxels, and our regularized framework. The experiments demonstrate the advantages of the regularization from the learned global dictionary as well as the non-local smoothness regularizer.

4.1. Synthetic Dataset

We first evaluate the reconstruction performance with our synthetic data field using the simulation model proposed in [13] with cylindrical fiber radius of $5\mu m$, length $5mm$ and diffusion weighting $b=1500s/mm^2$. All the data were simulated using 81 gradient directions with different noise level δ changing from 0 to 0.3. We compared our results against both the voxel-wise reconstruction as well as voxel-wise reconstruction on the smoothed data field using the non-local mean denoising algorithm. For the individual adaptive kernel, we picked $N=321$, $P=5$, ψ_k to be a 3rd-order B-spline basis function. For our dictionary learning framework, we set dictionary size $D=100$, $T_0=4$, $\lambda=2\delta$ and $\mu=10\delta$ where δ can be estimated in real dataset. For NLM, we set the radius of local patch to be 3, the radius of neighbourhood search window to be 5. In our experiments, we observed the advantages of our method is not sensitive to choices of λ and μ.

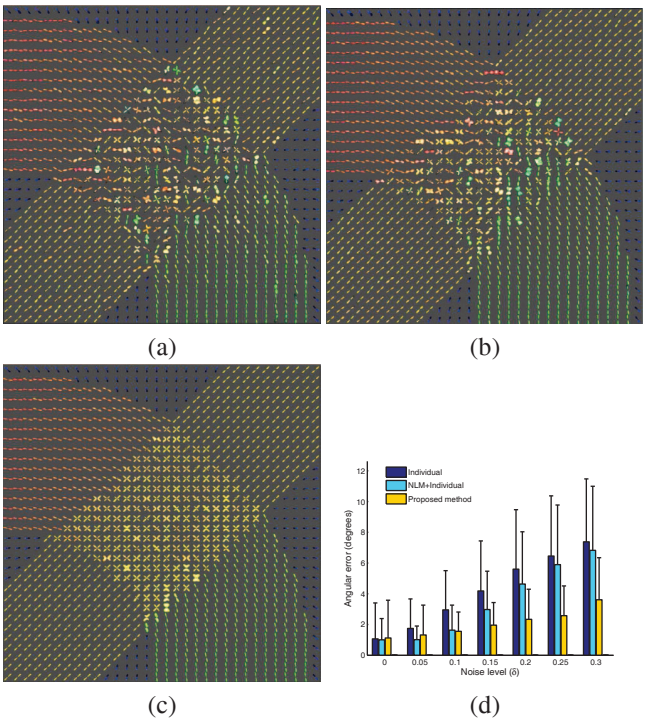


Fig. 1. Reconstructed field ($\delta=0.2$) using (a) voxel-wise individual reconstruction, (b) voxel-wise reconstruction on NLM denoised data field, (c) the proposed method. (d) shows the angular error for different δ.

The results show that the proposed method is much more accurate when the noise level is high since the voxel-wise reconstruction method does not take advantage of the smooth global fiber structure and is more vulnerable to the noise.

4.2. Real Dataset

We also performed an evaluation of the proposed method with real data from a rat optic chiasm, which contains samples measured with 46 different directions with b-value around

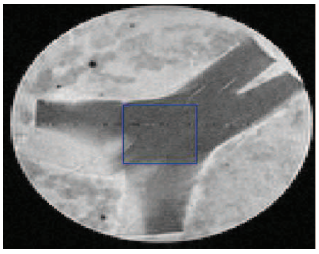
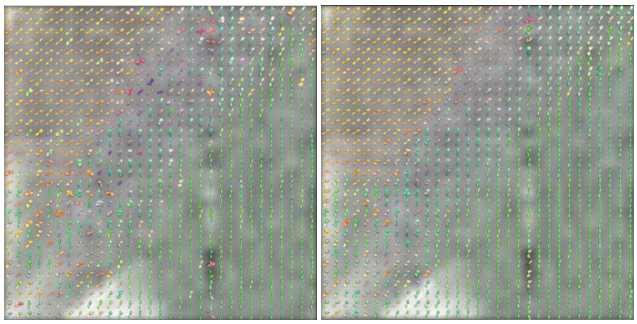


Fig. 2. S_0 image of the optic chiasm and the ROI.

$1240s/mm^2$. The S_0 image as well as the region of interest, marked with a blue box, are shown in Figure 2. The reconstructed $P(\boldsymbol{r})$ field at the region of interest is shown in Figure 3. We observe that the proposed method generates a smooth reconstruction while keeping the underlying fiber structure. The parameter setting is the same as those used in the synthetic experiments except that we picked a different value of $T_0 = 12$ and estimated the value of $\delta = 0.17$ from the homogeneous (noisy) areas of the image.



(a) (b)

Fig. 3. Reconstructed region of interest using (a) voxel-wise individual reconstruction, (b) the proposed method.

5. CONCLUSION

We proposed a novel EAP reconstruction framework based on dictionary learning that allows us to improve the reconstruction with a non-local regularization. This method reconstructs the whole field of EAPs. Through learning a dictionary from the given data volume and enforcing the regularization, our approach generates reconstructions at voxels that are robust to noise and preserve fiber structures at the same time. The advantages are shown through both synthetic and real data experiments.

References

[1] P. T. Callaghan, *Principles of Nuclear Magnetic Resonance Microscopy*, Clarendon Press, Oxford, 1991.

[2] P. J. Basser, J. M., and D. LeBihan, "Estimation of the effective self-diffusion tensor from the NMR spin echo.," *J. Magn. Reson., Ser B*, vol. 103, pp. 247–254, 1994.

[3] D. S. Tuch, T. G. Reese, M. R. Wiegell, N. Makris, J. W. Belliveau, and V. J. Wedeen, "High angular resolution diffusion imaging reveals intravoxel white matter fiber heterogeneity," *MRM*, vol. 48, no. 4, pp. 577–582, 2002.

[4] E. Özarslan, T. M. Shepherd, B. C. Vemuri, S. J. Blackband, and T. H. Mareci, "Resolution of complex tissue microarchitecture using the diffusion orientation transform (DOT)," *NeuroImage*, vol. 31, pp. 1086–1103, 2006.

[5] M. Descoteaux, R. Deriche, D. Le Bihan, J.F. Mangin, and C. Poupon, "Diffusion Propagator Imaging: Using Laplace's Equation and Multiple Shell Acquisitions to Reconstruct the Diffusion Propagator," in *IPMI*, 2009, pp. 1–13.

[6] W. Ye, S. Portnoy, A. Entezari, B.C. Vemuri, and S.J. Blackband, "Box spline based 3d tomographic reconstruction of diffusion propagators from mri data," in *ISBI*. IEEE, 2011, pp. 397–400.

[7] B. Jian and B.C. Vemuri, "A unified computational framework for deconvolution to reconstruct multiple fibers from diffusion weighted MRI," *TMI*, vol. 26, no. 11, pp. 1464–1471, 2007.

[8] O. Michailovich, Y. Rathi, and S. Dolui, "Spatially regularized compressed sensing for high angular resolution diffusion imaging," *TMI*, vol. 30, no. 5, pp. 1100–1115, 2011.

[9] J. D. Tournier, F. Calamante, D. G. Gadian, and A. Connelly, "Direct estimation of the fiber orientation density function from diffusion-weighted MRI data using spherical deconvolution," *NeuroImage*, vol. 23, no. 3, pp. 1176–1185, 2004.

[10] A. Barmpoutis, B. Jian, and B. C. Vemuri, "Adaptive kernels for multi-fiber reconstruction," in *IPMI*, July 2009, pp. 338–349.

[11] M. Aharon, M. Elad, and A. Bruckstein, "K-SVD: An algorithm for designing overcomplete dictionaries for sparse representation," *TSP*, vol. 54, no. 11, pp. 4311–4322, 2006.

[12] A. Buades, B. Coll, and J.M. Morel, "A non-local algorithm for image denoising," in *CVPR*. IEEE, 2005, vol. 2, pp. 60–65.

[13] O. Söderman and B. Jönsson, "Restricted diffusion in cylindrical geometry," *J. Magn. Reso., Ser A*, vol. 117, no. 1, pp. 94–97, 1995.